

Project Number: BC-KNW-0031

PERTURBATION ANALYSIS OF A POTASSIUM CHANNEL BETA SUBUNIT

A Major Qualifying Project Report:

submitted to the Faculty

of the

WORCESTER POLYTECHNIC INSTITUTE

in partial fulfillment of the requirements for the

Degree of Bachelor of Science

by

Elisabeth A. Jansizewski

27 April 2006

Approved:

Prof. Kristin Wobbe, Advisor

Abstract:

KCNQ1 is a voltage-gated potassium channel that co-assembles with the KCNE family of transmembrane peptides. KCNQ1/KCNE3 channels are found in colonic crypt and airway epithelial cells and are constitutively conducting at normal resting potentials. Using site-directed mutagenesis, residues 87-96 in the C-terminus were mutated to alanine. The RNA of these mutants was microinjected into *Xenopus* oocytes and examined using a two-electrode voltage clamp. Results were compared to KCNE1 to determine the role of C-terminus in KCNQ1 modulation.

Acknowledgments:

I wish to thank Steven Gage, Jessica Rocheleau and Trevor Morin for their help with the experimental aspects of this project. Also, the support and encouragement from Kshama Chandrasekhar, Tuba Bas and Andrew Driscoll was appreciated. Most importantly, I wish to acknowledge the work of my advisors, Dr. William Kobertz and Professor Kristin Wobbe, without whose positive words, constant support and helpful advice this project would not have been completed.

Table of Contents

Abstract	2
Acknowledgements	3
1 Introduction	5
2 Background	
2.1 Voltage Gated Potassium Channels	6
2.2 KCNQ1 Voltage Gated Channel	8
2.3 KCNQ1/KCNE3 Channels	9
2.4 Perturbation Analysis of Kv Channels	10
3 Materials and Methods	
3.1 Cloning of KCNE3 Gene	12
3.2 KCNE3 Mutants	12
3.3 In Vitro RNA Transcription	14
3.4 Oocyte Extraction and RNA Injection	14
3.5 Electrophysiological Recordings	15
3.6 Data Analysis	16
4 Results	
4.1 KCNE3 Clones and Mutants	17
4.2 Electrophysiology and Ratio Optimization	18
4.3 Data Analysis	20
5 Discussion	21
References	22

1 Introduction

Voltage gated potassium channels (Kv channels) play important physiological roles in all forms of life. Kv channels can repolarize cells, help maintain resting membrane potential or drive secretion of other ions such as sodium and chloride. Kv channels open and close in response to changes in membrane potential, thereby regulating the flow of potassium in and out of the cells (Voet, Biochemistry, 2004).

KCNQ1 is a Kv channel with six transmembrane helices, and one pore loop. KCNQ1 partners with a variety of subunits, including all five members of the KCNE family. KCNE peptides are believed to have one transmembrane domain, with the N-terminus on the extracellular side of the membrane, and the C-terminus on the intracellular side of the membrane. KCNE peptides regulate gating kinetics and function of KCNQ1 channels, as well as other Kv channels, and account for the variety of currents observed in vivo (Robbins, 2001).

In the human heart, KCNQ1/KCNE1 complexes form the slow-activating outward I_{KS} currents. Mutations in KCNE1 and KCNQ1 lead to Long QT syndrome, which slows the repolarization of the heart and may lead to deadly cardiac arrhythmia. (Abbott and Goldstein, 2001) In colonic crypt cells, KCNQ1/KCNE3 complexes form a channel complex that is open at the large negative resting potentials of the cells, activates quickly and has a linear I/V relationship, unique from KCNQ1/KCNE1 complexes. The KCNQ1/KCNE3 complex may play a role in driving chloride secretion (Schroeder et al, 2000).

While the role of voltage-gated potassium channels is well understood, the protein-protein interactions that generate these roles are less well understood. One method of identify protein-protein interactions is perturbation analysis. Perturbation analysis of potassium channels has proved useful in identifying structures and protein-protein interfaces. Comparison of electrophysiological data to that of wild-type channels will yield high impact and low impact amino acid residues; high impact residues may indicate protein-protein interactions (Hong and Miller, 2000; Li-Smerin et al, 2000). Similar methods can be employed to study structure and function of Kv channel subunits.

2 Background

Understanding the complex role potassium channels and their subunits play in human physiology is necessary for justifying further study of these proteins. Much of the knowledge surrounding KCNQ1 and KCNE3 has come to light in recent years, and many questions are still left unanswered. Comparisons to other voltage-gated potassium channels may aid in explanation of observed behavior of KCNQ1/KCNE3 complexes.

2.1 Voltage Gated Potassium Channels

Ion channels serve the role in cells of maintaining resting membrane potential. One type of ion channel, voltage gated channels, open or close in response to changes in the membrane potential of the cell. Voltage gated potassium channels are a large family of proteins widely distributed in most forms of life (Abbott and Goldstein, 1998). Structurally, this family is characterized by a tetramer of subunits. Each subunit contains one P-loop and six transmembrane (TM) domains. Four P-loops surround a water-filled pore in the membrane, through which the potassium moves (Abbott and Goldstein, 1998). The six TM domains (called S1-S6) enclose the pore (See figure 1). One TM domain, S4, contains five positively charged amino acid residues, which are thought to sense voltage changes (Voet, Biochemistry, 2004).

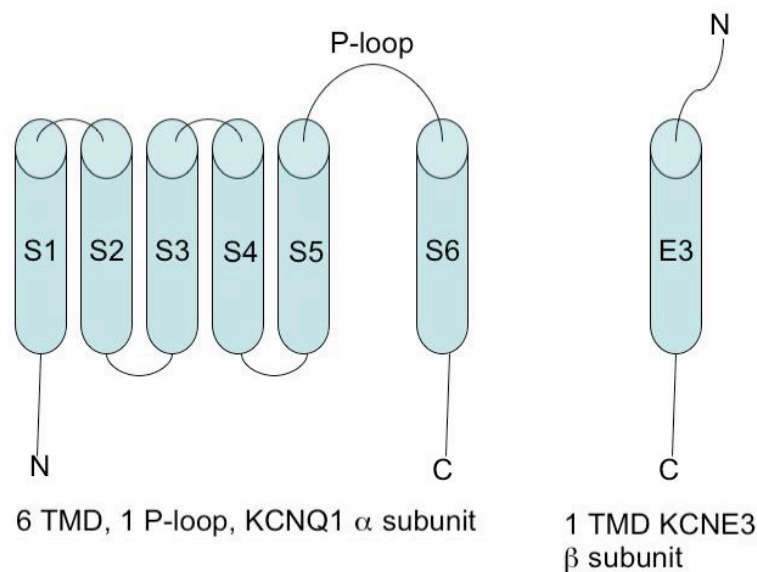


Figure 1 - Basic structure of Kv subunits

Kv channels in mammals are often found to have accessory subunits associated with them. Cytoplasmic, peripheral and integral membrane proteins can all function as subunits that regulate, stabilize or inactivate Kv channels. Integral membrane proteins typically assemble with the Kv channel to create native currents, therefore accounting for the diversity of kinetics observed with Kv channels (Abbott and Goldstein, 1998).

The crystal structure of a mammalian Kv channel, Kv1.2, was crystallized by Long, Campbell and MacKinnon (2005). Kv1.2 was crystallized with a peripheral β subunit. The structure showed four subunits of helices S1-S6 in a tetramer. The S5 and S6 helices of one subunit overlap the S4-S5 linker of another subunit. Within the ion conduction pore, on the S6 helix, the Pro-X-Pro sequence is conserved among Shaker-family Kv channels, but is not seen in prokaryotic Kv channels. In the crystal structure, the Pro-X-Pro sequence gives a kink to the S6 helix. This shape is also seen in prokaryotic channels with a Gly residue and may play a role in ion selectivity (Long et al, 2005) (See Figures 2A and 2B).

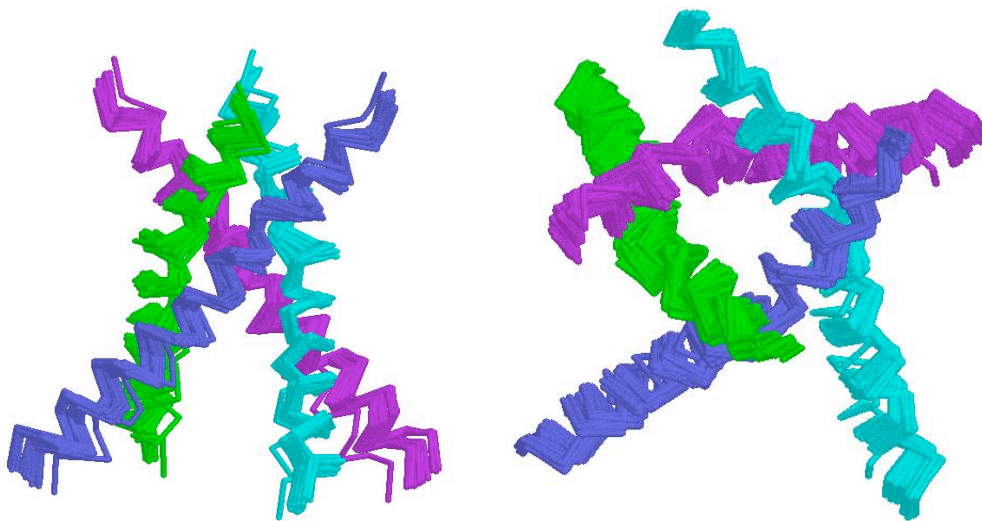


Figure 2A and B - KcsA prokaryotic K channel side view and top view

2.2 KCNQ1 Voltage Gated Channel

The KCNQ family of Kv channels has six TMD and 1 P-loop domain. KCNQ channels form both homotetramers and heterotetramers. Mutations in members of the KCNQ family have been linked to a variety of human diseases; some pharmacological chemicals have been shown to have particular affinity for individual members of the KCNQ family as well. (Robbins, 2001) One member of this family, KCNQ1, has been found in many tissues, including cardiac muscle, skeletal muscle, intestinal cells and the ear (Abbott and Goldstein, 1998; Schroeder et al, 2000). In the heart, KCNQ1 assembles with five members of the KCNE family of subunits. These subunits consist of one transmembrane domain (See Figure 1) and regulate the currents of KCNQ1, as well as other Kv channels. (McCrossan and Abbott, 2004). In the human heart, KCNQ1 assemblies with KCNE1, KCNE2 and KCNE3 are believed to create the I_{KS} repolarization currents which are essential for normal cardiac function. Mutations in KCNE1 have been linked to Long QT Syndrome and atrial fibrillation (Abbott and Goldstein, 1998), as well as deafness.

KCNQ1 homomers are sensitive to a variety of compounds. Tetraethylammonium (TEA), linopirdine, XE991, Chromonal 293B and Clofillium all inhibit KCNQ1 at a predictable level. Assembly with KCNE peptides can alter pharmacology of the channels and can be used to study channel properties (Robbins, 2001). KCNQ1 channels also display inactivation which can be readily observed in high potassium solutions. Seeböhm et al (2003) claim that this inactivation is due to a “fast flickery process” between two different open states of the channel. This same gating mechanism is proposed to influence conductance of rubidium, due to a larger pore size allowing Rb^+ ions to pass as well as giving rise to Na^+ block. Assembly of KCNQ1 with KCNE peptides has been shown to alter inactivation and Rb^+ conductance but not Na^+ discrimination. Because of this, Seeböhm et al (2003) claim that KCNE peptides influence only one open state, which in turn effects the fast flickery movement between states in KCNQ1. While this data suggests possible sites of interaction between KCNE peptides and KCNQ1, no definitive evidence has surfaced.

2.3 KCNQ1/KCNE3 Channels

KCNQ1/KCNE3 channels are found in human heart, as well as colonic crypt cells and airway epithelial cells (Schroeder et al, 2000). KCNQ1 alone, as well as KCNQ1/KCNE1 channels would not be open at the negative resting potentials of these epithelial cells, however KCNQ1/KCNE3 channels would be open at this voltage. The KCNQ1/KCNE3 channels produce characteristic currents that are almost instantaneously open upon stimulation and have a linear I/V ratio (Schroeder et al, 2000). Expression in *Xenopus laevis* oocytes of KCNQ1/KCNE3 reproduced the currents observed in the colonic cells (Schroeder et al). KCNQ1/KCNE3 channels may be implicated in colonic chloride transport, because the channel removes K^+ that was initially transported by the NaK2Cl channel, which in turn hyperpolarizes the cell, potentially stimulating the CFTR chloride transporter to open, so chloride ions can leave the cell. Studies have shown that KCNQ1/KCNE3 channels may be cAMP-activated (Schroeder et al, 2000). See Figure 3 for peptide sequence of KCNE3.

Studies of KCNE1 and KCNE3 complexed with KCNQ1 done by Melman et al (2002) suggest that a triplet of amino acids are necessary for functional specificity. Moreso, the central amino acid—Thr58 in KCNE1 and Val72 in KCNE3—specifically controls the voltage gating properties (Melman et al, 2002). Melman et al (2002) found that substitution of an aliphatic amino acid at the Thr-58 position in KCNE1 produced KCNE3-like currents. Similarly, substitution of an amino acid with a hydroxyl group for the Val residue at position 72 in KCNE3 produces KCNE1-like currents. This data suggests that the only amino acids necessary for modulation of KCNQ1 by KCNE1 or KCNE3 occur within the triplet (Melman et al, 2002). However, this is contrary previous studies with KCNE1, where mutations near the COOH terminus are found to cause Long QT syndrome.

Gage and Kobertz (2004) proposed a bipartite model for modulation of KCNQ1 by KCNE3. Truncation mutants of the NH₂ terminus, so long as they contained glycosylation sites, were sufficient to regulate KCNQ1 currents similar to wild-type (WT) KCNE3. Truncation mutants of the COOH terminus exhibit similar characteristics to WT KCNE3, however inactivation, slow kinetics and lowered expression were observed. Double truncation mutants, which essentially contained only the

transmembrane (TM) portion of KCNE3, exhibited similar characteristics to COOH terminus truncations. Also, the COOH terminus mutation D90N—analogue to LQTS-causing mutation in KCNE1 D76N—was masked by a functional TM domain. Additionally, chimeras of KCNE1 D76N and functional KCNE3 TM domain were also functional, however displayed slower kinetics as well as inactivation. Using chromanol 293B, which blocks KCNQ1 and KCNQ1/KCNE3 at different concentrations, it was shown that COOH terminus truncation mutants allow some KCNQ1 to reach the cell membrane alone. Gage and Kobetz’s data suggests that, while the TM domain is sufficient for channel regulation, the COOH terminus is important in trafficking. In KCNE3, the TM domain is more active in modulation, and overrides the COOH terminus modulation of KCNQ1, however in KCNE1 the TM domain is passive, therefore COOH terminus modulation is apparent in such cases as D76N.

METTNGTETWYESLHAVLKALNATLHSNLLCRPGPGLGPDNQTEERRASLPGRDDNSYMYILFVMFLFAVT
VGSLILGYTRSRVKRSDPYHVYIKNRVSMI

Figure 3 - KCNE3 peptide sequence. Green residues are nonpolar, cyan residues are polar, red residues are negatively charged, blue residues are positively charged, orange residues are helix breakers, black residues are histidine. TM segment is underlined.

2.4 Perturbation Analysis of Kv Channels

Perturbation analysis can be used to determine if a helical structure is present in a protein. Mutant impact can be measured electrophysiologically and compared to WT data in order to determine high and low impact residues. These residues are plotted on a helical wheel to determine if a pattern emerges. Large, bulky residues—such as Trp—will significantly alter channel function if that amino acid is in contact with any other part of the protein (Hong and Miller, 2000). A study done on the S1 and S3 regions of a Shaker K⁺ channel employed the tryptophan-scanning method. Each residue was individually mutated to Trp, then electrophysiological kinetics were measured, and a $\Delta\Delta G$ was determined. From this data, “high” and “low” impact residues were determined and plotted on a helical wheel. Analysis of this data showed the S1 segment to have a helical pattern. When a similar method was applied to the S3 region, only the first 14

residues showed a helical pattern; therefore, it is possible that the S3 region contains a helix as well as another structural motif (Hong and Miller, 2000).

Another possible method of perturbation analysis of Kv channels is through alanine scanning. Alanine scanning can be considered less invasive or likely to cause improper folding compared to tryptophan scanning (Li-Smerin et al, 2000). However, the principle is similar to tryptophan scanning, in that the small alanine residue will alter kinetics due to protein-protein interactions, and be relatively harmless at protein-water or protein-lipid interfaces. An alanine scan of *drkl* K⁺ channel S1-S4 segments revealed partial helical structures in all four segments, as well as small aqueous helical connecting loops (Li-Smerin et al, 2000). The perturbation data corroborated hydrophobic and secondary structure predictions for the segments. The recent high resolution structure of Kv1.2 (MacKinnon et al, 2005) validated the conclusions from perturbation analyses.

Because the KCNQ1/KCNE3 complex has known gating properties, a perturbation analysis of KCNE3 could be done in order to determine the structure of this subunit, as well as the portion of the peptide that interacts with KCNQ1. Similarly, electrophysiological methods (see Figure 4) could be applied in order to explore the secondary structure of KCNE3. Comparison of analogous residues in KCNE1 to those in KCNE3 may reveal important differences in KCNE3 and KCNE1 modulation of KCNQ1.

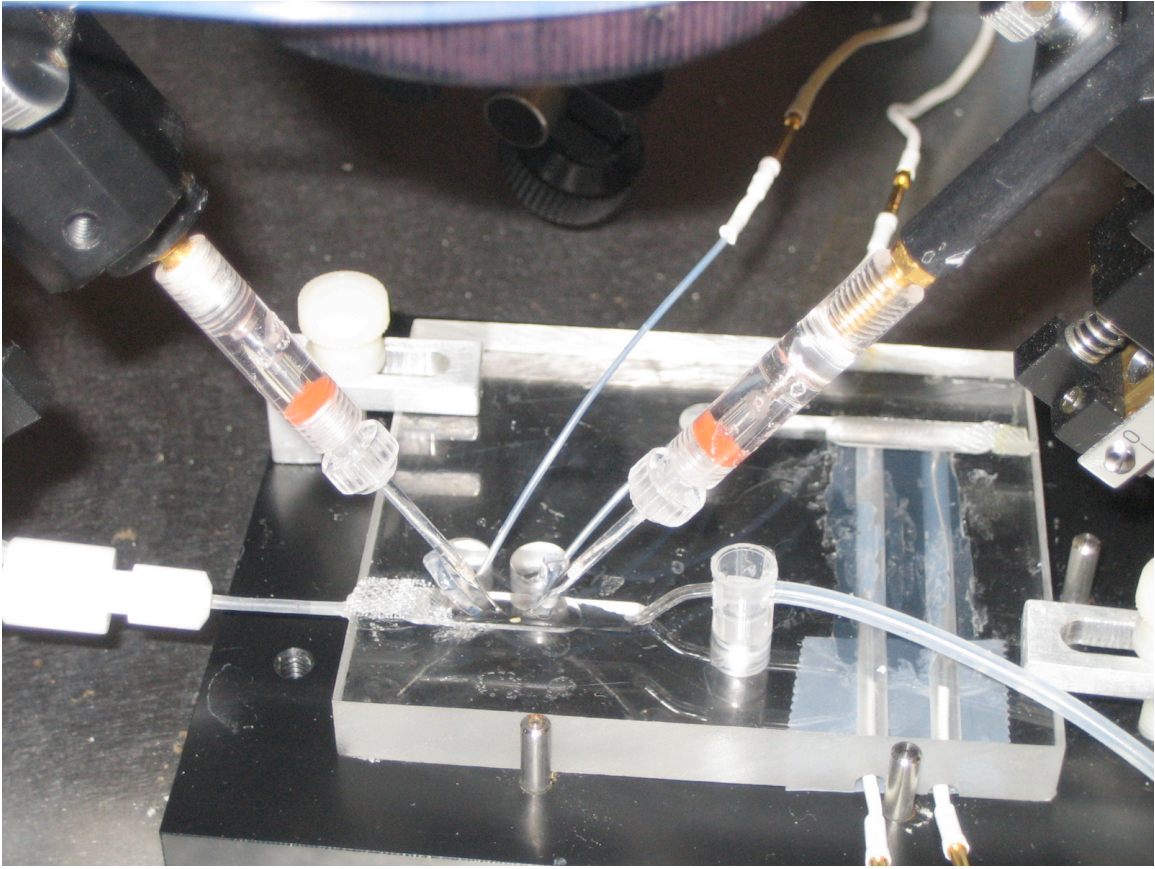


Figure 4 - Standard two electrode voltage clamp setup for oocyte recordings.

3. Materials and Methods

3.1 Cloning the KCNE3 Gene

The human KCNE3 gene was cloned using polymerase chain reaction with HotStarTaq, KCNE3 primer and primer 5203. Using a MJ Research PTC-200 thermocycler, the samples were heated for initial activation 15 minutes at 95°C, then 30 cycles of denaturing 1 minute 94°C, annealing 1 minute 55°C and extension 1 minute 72°C, with a final extension for 10 minutes 72°C. Samples were stored at 4°C then purified on 1.5% agarose gel. The insert band was cut out and purified using Qiagen QiaQuick PCR product purification system, then digested using HindIII and BglII (New England Bioscience) restriction enzymes. Inserts were purified using QiaQuick system (Qiagen). The digested insert was ligated into the pSG01MX vector using T4 DNA Ligase (2,000,000 U). XL Blue Supercompetant E. coli cells were transformed with the ligation mix and plated on LB agar plates containing either carbanicillian or ampicillian (1 mg/ml final concentration). Plates were incubated overnight at 37°C. Individual colonies were then isolated and incubated overnight in liquid cultures containing LB broth and carbanicillian or ampicillian on a shake table (225 RPM). Liquid cultures were then centrifuged 10 minutes at 5000 RPM. The pellet was resuspended in Sigma Miniprep Suspension Solution (Sigma). The plasmid was isolated using Sigma Miniprep Kit (Sigma). NcoI test digests were performed to determine correct insertion and run on 1% agarose gel, then sequence was determined by automated sequencing.

3.2 KCNE3 Mutations

Mutations were introduced using a cloning cassette method employing two step PCR and mutagenic primers (See Table 1). Custom primers were from Sigma Geno-Sys.

Primer Name	Sequence (5' – 3')
K87Aa	CTAGAAAAGTGGACGCGCTAGTGACCCCTATC
K87Ab	GATAGGGGTCCTACTACGCGCTCCACTTTTCTAG
R88Aa	CTAGAAAAGTGGACAAGGCTAGTGACCCCTATC
R88Ab	GATAGGGGTCCTACTAGCCTTGTCCTACTTTTCTAG
S89Aa	GAAAAGTGGACAAGCGTGCTGACCCCTATCATGTG
S89Ab	CACATGATAGGGGTCAGCACGCTTGTCCTACTTTTTC
D90Aa	GTGGACAAGCGTAGTGCCCCCTATCATGTGTATATC
D90Ab	GATATACACATGATAGGGGGCACTACGCTTGTCAC
P91Aa	GGACAAGCGTAGTGACGCTTATCATGTGTATATC
P91Ab	GATATACACATGATAGGGGTCCTACTACGCTTGACC
Y92Aa	TGGACAAGCGTAGTGACCCCGCTCATGTGTATATCAAGAAACG
Y92Ab	CGTTTCTTTGATATACACATGAGCGGGGTCCTACTACGCTTGTC
H93Aa	CAGCGTAGTGACCCCTTATGCTGTGTATATCAAGAAC
H93Ab*	GTTCCTTGATATACACAGCATAAGGGTCACTACCGAC
V94Aa	GTGACCCCTATCATGCGTATATCAAGAACCGT
V94Ab	ACGGTTCTTTGATATACGCATGATAGGGGTCAC
Y95Aa	GACCCCTATCATGTGGCTATCAAGAACCGTG
Y95Ab	CACGGTTCTTTGATAGCCACATGATAGGGGTC
I96Aa	CCCCTATCATGTGTATGCCAAGAACCGTGTGT
I96Ab	ACACACGGTTCTTTGGCATAACATGATAGGGG

Table 1 - Mutagenic PCR primers for KCNE3. The * indicates a silent mutation present in order to prevent primer dimer.

The PCR protocol is as follows:

PCR 1a:

2 ng of KCNE3 template DNA was mixed with 50 uM of T7 primer, mutagenic primer “b” and TaqHotStart. For mutant H93A, 6% DMSO was added.

PCR 1b:

2 ng of KCNE3 template DNA was mixed with 50 uM of 5203 primer, mutagenic primer “a” and TaqHotStart. For mutant Y95A, 6% DMSO was added.

PCR 1a and 1b were run for 15 minutes at 94°C, and 30 cycles total of 1 minute at 94°C, 1 minute at 55°C, and 1 minute at 72°C, then 10 minutes at 72°C. Samples were stored at 4°C until further steps were taken. For mutant H93A, annealing was preformed at 65°C. Samples were run on 2% agarose gel. Samples were diluted 1:10 and 1:100 for use in PCR step 2. Diluted samples were mixed with 200 uM T7 primer and 200 uM 5203 primer, and TaqHotStart. The same heat cycle was used as in PCR 1a and 1b. Samples were analyzed on 2% agarose gel, and bands were cut out and purified using Qiagen QiaQuick purification. Digestion with HindIII and BglII, ligation, plasmid preparation and NcoI test digests were performed as with KCNE3 clones.

3.3 In Vitro RNA Transcription

4-6 ng of KCNE3, KCNE3 mutants and KCNQ1 DNA was linearized using MluI (New England Biosciences) then extracted with 1:1 phenol:chloroform and precipitated at -80°C with ethanol. RNA was transcribed using run off transcription with either T7 Polymerase (KCNE3 and mutants) or SP6 Polymerase (KCNQ1). RNA was extracted with 1:1 phenol:sevag and precipitated with isopropanol on ice. RNA was resuspended in RNase-free water, run on 1.5% agarose gel and stored at -80°C.

3.4 Oocyte Extraction and RNA Injection

Oocytes were surgically removed from anesthetized *Xenopus laevis*. The oocyte sacs were mechanically separated using tweezers then incubated in OR2 (in mM: 8.25 NaCl, 2 KCl, 1 MgCl₂, 5 HEPES, pH 7.4 using NaOH) with 2 mg/ml collagenase type II (Worthington Biochemicals) for 75 minutes at room temperature. Defolliculated oocytes were stored at 16°C in ND96 High Calcium (in mM: 96 NaCl, 2 KCl, 1.8 CaCl₂, 1 MgCl₂, 5 HEPES, pH 7.6 using NaOH) with 50 µg/ml Gentamicin (Sigma Aldrich).

One day after removal, healthy oocytes were injected with RNA using a microinjector (See Figure 5). The ratios for KCNQ1: KCNE3 were empirically determined. Oocytes were injected first with 7.5 ng KCNQ1 and 4.5 ng KCNE3 and mutants, then with 4.5 ng KCNQ1 and 6.5 ng KCNE3 and mutants. Injected oocytes were stored at 16°C in ND96 High Calcium and 50 mg/ml Gentamicin for 2-5 days.

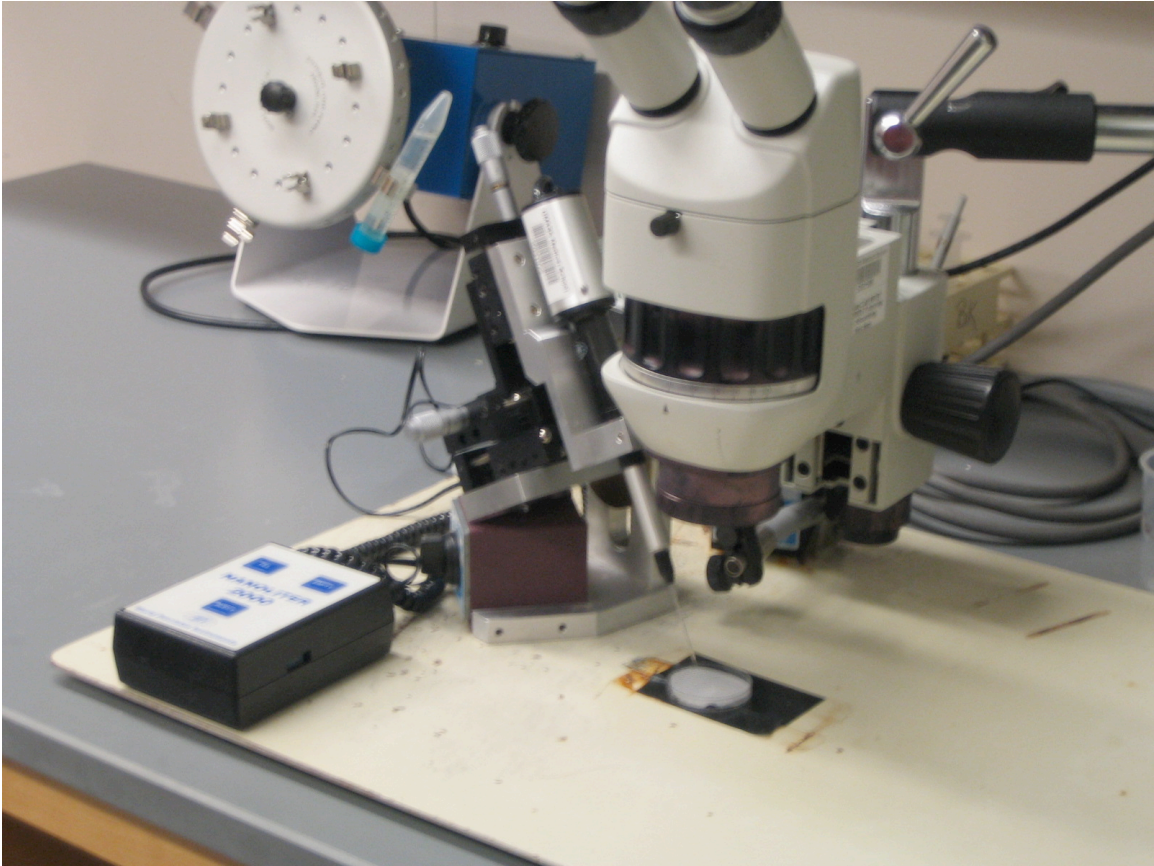


Figure 5 - Microinjection Setup

3.5 Electrophysiological Recordings

Two to three days post injection, oocytes were selected for electrophysiology. Oocytes were voltage clamped using two-electrode voltage clamp setup (Axon Instruments DigiData 1322A and Warner 750C Oocyte clamp) at -80 mV in ND96 Recording (In mM: 96 NaCl, 2 KCl, 0.3 CaCl₂, 1 MgCl₂, 5 HEPES, pH 7.6 with NaOH). Currents were recorded using Clampex9.2 program. Currents were elicited starting at -100 mV, to $+60$ mV in steps of 20. The interpulse interval was 20 seconds. The oocytes were then bathed in KD98 (in mM: 98 KCl, 0.3 CaCl₂, 1 MgCl₂, 5 HEPES, pH 7.6 with NaOH) and currents were elicited from -100 mV to $+80$ mV in steps of 10. Oocytes were then returned to ND96 solution, and currents were elicited at 0 mV, $+20$ mV, $+60$ mV to confirm oocyte health.

3.6 Data Analysis

Tail currents were measured 3–6 ms after the capacitive transient using Axon Instruments Clampfit. Using Microcal Origins Professional 6.0, currents were normalized to I_{\max} . An I/V curve was generated, and fitted using the Boltzmann Function:

$$y=A1+(A2-A1)/(1+\exp((V- V_{1/2})(-0.0393*z)))$$

ΔG was calculated from the equation zVF , where z is the maximal slope, $V_{1/2}$ is the midpoint of voltage-activation, and F is Faraday's constant.

$\Delta\Delta G$ is generated by:

$$\Delta G_{\text{mutant}} - \Delta G_{\text{WT}}$$

Standard error of the measurement was also calculated.

4 Results

4.1 KCNE3 Clones and Mutants

In order to carry out site-directed mutagenesis, it was first necessary to clone human KCNE3 into the pSG01MX plasmid, which is usable in both *Xenopus* oocytes and mammalian cell lines. Once cloned into pSG01MX, KCNE3 was used as a template for cassette cloning. See Figure 6. PCR of KCNE3 yielded a band with a length of approximate 394 bases. PCR 1a of the mutants yielded a band of approximately 300 bases, and PCR 1b a band of approximately 100 bases. See Figure 7. PCR 2 yields a band of approximately 400 bases. After digestion, NcoI tests digests were performed. KCNE3 inserts were compared to pSG01MX with E1, while KCNE3 mutants were compared to wild type KCNE3 in pSG01MX. See Figure 8. After a successful NcoI digest, mutants were confirmed by sequencing the cloning cassette at UMass Medical School Nucleic Acid Facility.

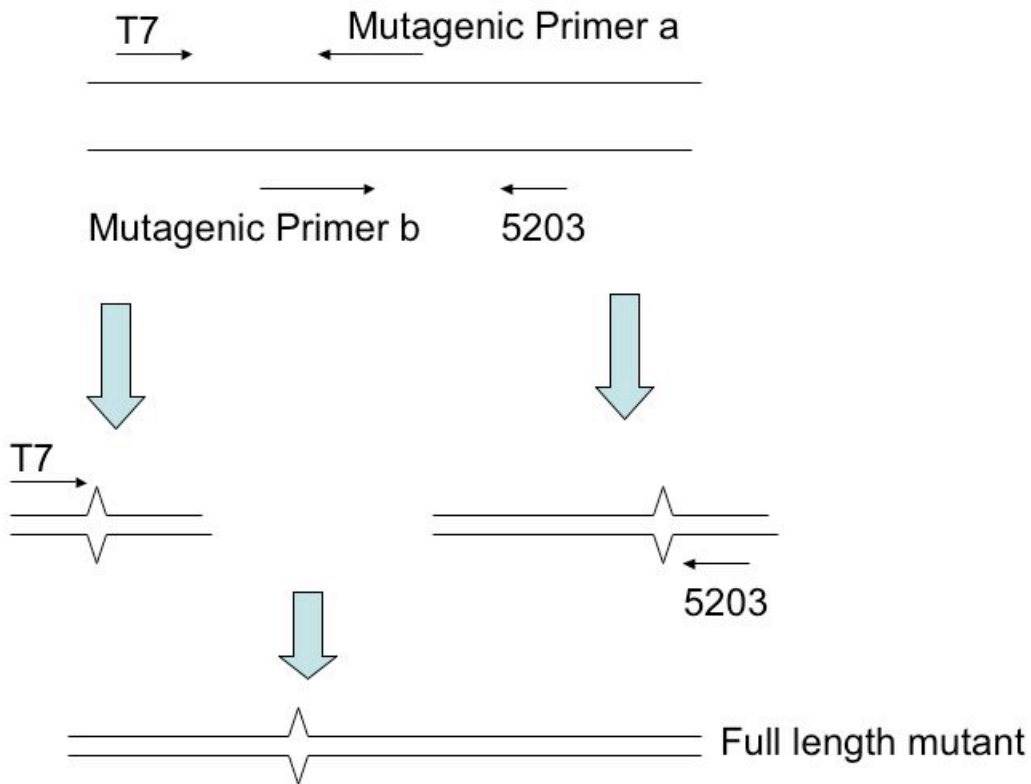


Figure 6 - PCR schematic for mutagenesis.

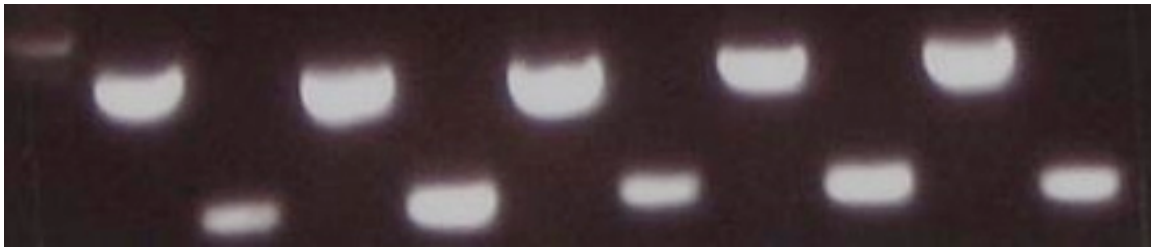


Figure 7 - 1.5% agarose gel of PCR 1 of KCNE3 mutants. Lanes from left to right: Marker; K87A 1a, 1b; R88A 1a, 1b; S89A 1a, 1b; D90A 1a, 1b; P91A 1a, 1b. Similar data was obtained for mutants Y92A, V94A, Y95A and I96A.



Figure 8 - NcoI test digest of mutagenized KCNE3 clones. Lanes from left to right: Marker, WT E3 in pSG01MX, K87A, R88A, S89A, D90A, P91A, Y92A, V94A, Y95A, I96A.

4.2 Electrophysiology and Ratio Optimization

Typically, ratios of RNA used in electrophysiology must be determined empirically. Effectiveness of ratios can vary due to quality of RNA, precision of injection and general oocyte health. In order to achieve ideal currents, ratios must be optimized for WT and each mutant for a given RNA. Previous work (Gage and Kobertz, 2005) provided guidelines for injection ratios. In general, oocytes injected with 7.5 ng KCNQ1 RNA and 3.75 ng KCNE3 WT RNA yielded currents lower than expected for KCNQ1/KCNE3 complexes. This is also generally true of the mutants R88A, S89A, D90A and V94A. Resting potentials before clamping were generally between -70 and -75 mV. Upon visual inspection of the family of traces, in low potassium, an inactivation was seen at $+40$ mV and $+60$ mV, characteristic of KCNQ1 alone. In addition, in high potassium, a KCNQ1 characteristic “hook” in the tail currents, also due to inactivation,

was clearly visible at higher voltages. In typical KCNQ1/KCNE3 complexes these artifacts of inactivation are generally not seen. This suggests that the currents observed at this ratio are due to assembly of KCNQ1 at sub-stoichiometric ratios of KCNE3 or presence of KCNQ1 channels without KCNE3.

Oocytes injected with 4.5 ng KCNQ1 RNA and 6.5 ng KCNE3 WT RNA exhibited currents at the level expected for KCNQ1/KCNE3 complexes. Before clamping, resting potentials were generally between -80 and -90 mV. Mutants R88A and Y95A also had resting potentials in this area. See Figure 9.

Mutants D90A, V94A and I96A were all injected at a ratio of 3 ng KCNQ1 RNA to 12 ng KCNE3 RNA. This ratio led to resting potentials before clamping of greater than -75 mV, and currents that resembled WT KCNE3 currents. See Figure 9. Mutants S89A, P91A and Y92A did not generate current in enough oocytes to study, most likely due to poor RNA quality not the mutation itself.

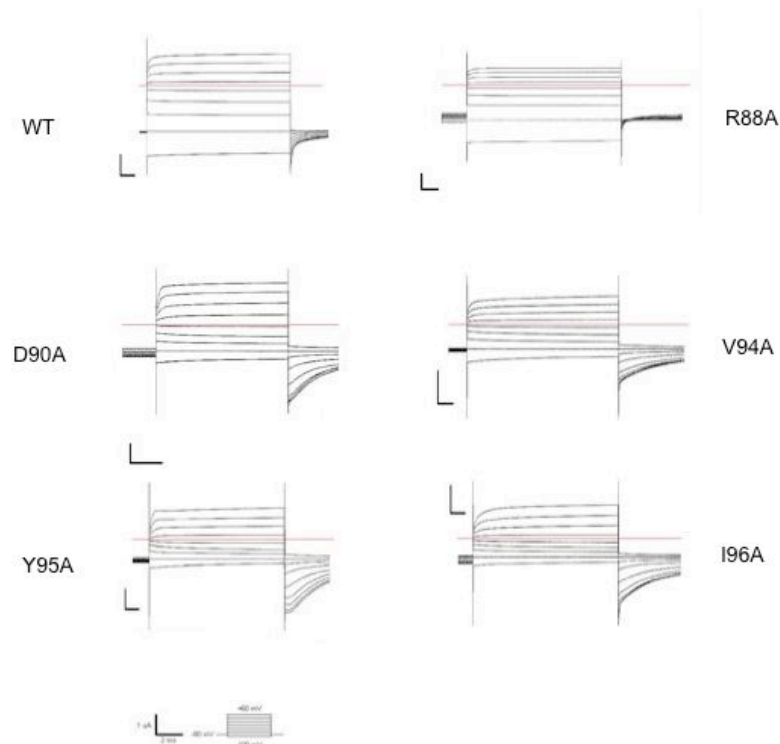


Figure 9 - Electrophysiological recordings in KD98 (high potassium). The red line indicates 0 mV. The pulse protocol is in the lower left column.

4.3 Data Analysis

Activation curves (normalized current vs. voltage) were generated for each mutant. Shown in Figure 10 is the WT activation curve, and the activation curve for D90A. Other activation curves were similar. After fitting the activation curves with a Boltzmann function, the data in Table 2 was generated.

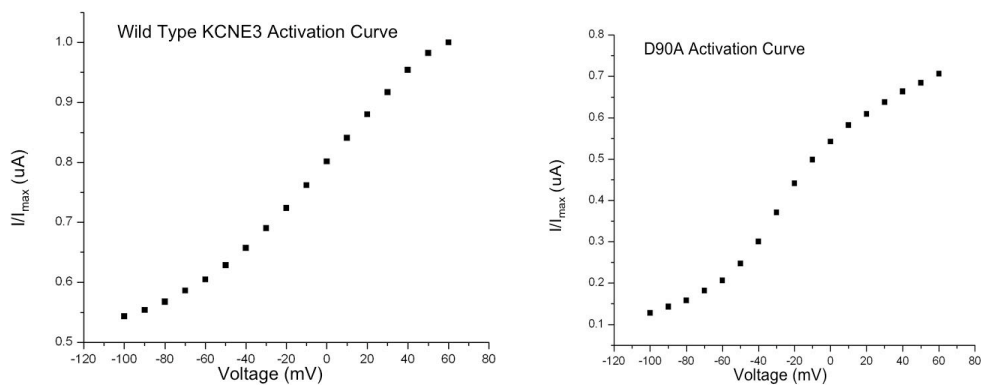


Figure 10 - Activation curves for WT and D90A.

	z (charge)	V_{1/2} (mV)	ΔG (kcal/mol)	ΔΔG (kcal/mol)
Wild Type (n=7)	1.05±0.12	-19.3±2.0	-0.47±0.07	
R88A (n=5)	0.92±0.09	-15.3±8.2	-0.33±0.17	0.14±0.19
D90A (n=3)	1.31±0.03	-27.2±2.1	-0.83±0.06	-0.36±0.09
V94A (n=3)	1.05±0.01	-28.0±4.2	-0.68±0.10	-0.21±0.12
Y95A (n=2)	1.36±0.22	-28.2±1.3	-0.88±0.15	-0.42±0.17
I96A (n=4)	1.09±0.06	-13.0±1.0	-0.33±0.03	0.14±0.07

Table 2 - Data generated from activation curves.

5 Discussion

Based on the data generated from the recordings and shown in Table 2, this region of the C-terminus does not impact modulation of KCNQ1 by KCNE3. Former work (Hong and Miller, 2000; J. Rocheleau, unpublished data) has shown that a $\Delta\Delta G$ of greater magnitude than 1 kcal/mol is indicative of a high impact residue; none of the mutants tested here generated a $\Delta\Delta G$ greater than 0.42 kcal/mol. Therefore, based on the small sample of C-terminus mutants studied, it appears that the C-terminus of KCNE3 does not impact modulation, in accordance with the previous truncation studies done by Gage and Kobertz (2004).

Of particular interest is mutant D90A. The analogous mutation in KCNE1 has been shown to generate non-functional complexes (Gage and Kobertz, 2004). However, this mutation in KCNE3 appears to not effect complex functionality in any significant way. The activation curve is slightly left-shifted, possibly due to presence of KCNQ1 channels without KCNE3; however, D90A is still a low-impact residue. This indicates that the C-terminus represents an area of significant difference in modulation between KCNE1 and KCNE3, despite amino acid conservation.

Further work is necessary in order to fully understand KCNE3 modulation of KCNQ1. Additional recordings of the mutants examined in this study would be beneficial in order to confirm statistical significance of the data. A tryptophan scan of the transmembrane region may provide insight into membrane-bound protein-protein interactions that effect modulation. Comparing data from KCNE3 perturbation analysis to that of KCNE1 may reveal important differences in modulation of these two related proteins.

References

1. Geoffery W. Abbott, Margaret H. Butler, Said Bendahhou, Marinos C. Dalakas, Louis J. Ptacek, Steve A. N. Goldstein. MiRP2 Forms Potassium Channels in Skeletal Muscle with Kv3.4 and Is Associated with Periodic Paralysis. *Cell*, Vol. 104, 217-231. January 26, 2001.
2. Geoffery W. Abbott, Steve A. N. Goldstein. A superfamily of small potassium channel subunits: form and function of the MinK-related peptides (MiRPs). *Quarterly Reviews of Biophysics*. Vol 31, 357-398. 1998.
3. Geoffery W. Abbott, Steve A. N. Goldstein. Disease-associated mutations in KCNE potassium channel subunits (MiRPs) reveal promiscuous disruption of multiple currents and conservation of mechanism. *The FASEB Journal*, Vol 16, 390-400. 2002.
4. Steven D. Gage, William R. Kobertz. KCNE3 Truncation Mutants Reveal a Bipartite Modulation of KCNQ1 K⁺ Channels. *Journal of General Physiology*. Vol 124. 759-771. December 2004.
5. Kwang Hee Hong, Christopher Miller. The Lipid-Protein Interface of a *Shaker* K⁺ Channel. *Journal of General Physiology*, Vol 115, 51-58, January 2000.
6. Yingling Li-Smerin, David H. Hackos, Kenton J. Swartz. α -Helical Structural Elements with the Voltage-sensing Domains of a K⁺ Channel. *Journal of General Physiology*. Vol. 115, 33-49, January 2000.
7. Stephen B. Long, Ernest B. Campbell, Roderick MacKinnon. Crystal Structure of a Mammalian Voltage-Dependant *Shaker* Family K⁺ Channel. *Science*, Vol 309, 897-902, 5 August 2005.
8. Zoe A. McCrossan, Geoffrey W. Abbott. The MinK-related peptides. *Neuropharmacology*, Vol 47, 787-821, 18 June 2004.
9. Yonathan F. Melman, Andrew Krummerman, Thomas V. McDonald. A Single Transmembrane Site in the KCNE-encoded Proteins Controls the Specificity of KvLQT1 Channel Gating. *Journal of Biological Chemistry*, Vol. 277, 25187-25194, 2002.
10. Jon Robbins. KCNQ potassium channels: physiology, pathophysiology and pharmacology. *Pharmacology & Therapeutics*, Vol. 90, 1-19, 2001.
11. Bjorn C. Schroeder, Siegfried Waldegger, Susanne Fehr, Markus Bleich, Richard Warth, Rainer Greger, Thomas J. Jentsch. A constitutively open potassium channel formed by KCNQ1 and KCNE3. *Nature*, Vol. 403, 196-199, January 2000.

12. Guiscard Seeböhm, Michael C. Sanguinetti, Michael Pusch. Tight coupling of rubidium conductance and inactivation in human KCNQ1 potassium channels. *Journal of Physiology*, Vol 552.2, 369-378, 2003.

13. Voet. Biochemistry, Third Edition. J. Wiley and Sons, 2004.